The influence of bulk evolution models on heavy-quark phenomenology

P. B. Gossiaux[1], S. Vogel[1], H. van Hees[2], J. Aichelin[1], R. Rapp[3], M. He[3], M. Bluhm[1*]
[1] *SUBATECH, UMR 6457, Laboratoire de Physique Subatomique et des Technologies Associées University of Nantes - IN2P3/CNRS - Ecole des Mines de Nantes 4 rue Alfred Kastler, F-44072 Nantes Cedex 03, France;*
[2] *Institut für Theoretische Physik, Universität Giessen, Heinrich-Buff-Ring 16, D-36392 Giessen, Germany;*
[3] *Cyclotron Institute and Department of Physics and Astronony, Texas A&M University, College Station, Texas 77843-3366, USA*
(Dated: February 6, 2011)

We study the impact of different Quark-Gluon Plasma expansion scenarios in heavy-ion collisions on spectra and elliptic flow of heavy quarks. For identical heavy-quark transport coefficients relativistic Langevin simulations with different expansion scenarios can lead to appreciable variations in the calculated suppression and elliptic flow of the heavy-quark spectra, by up to a factor of two. A cross comparison with two sets of transport coefficients supports these findings, illustrating the importance of realistic expansion models for quantitative evaluations of heavy-quark observables in heavy-ion collisions. It also turns out that differences in freeze-out prescriptions and Langevin realizations play a significant role in these variations. Light-quark observables are essential in reducing the uncertainties associated with the bulk-matter evolution, even though uncertainties due to the freeze-out prescription persist.

PACS numbers: 14.65.Dw, 25.75.Ld, 24.10.Nz, 24.85.+p

I. INTRODUCTION

One of the striking discoveries of the heavy-ion program at the Relativistic Heavy Ion Collider (RHIC) is that the medium created in 200 AGeV Au-Au collisions behaves like a nearly perfect liquid [1–8]. To further investigate this new state of matter, usually referred to as the Quark Gluon Plasma (QGP), penetrating and well calibrated probes are essential to quantitatively deduce the effect of the medium on those probes. One of these probes are heavy quarks. The experimental investigation of heavy-quark probes at RHIC has been ongoing for several years now [9, 10]. Two rather unexpected observations have emerged. Heavy mesons, despite their large mass, exhibit (a) an elliptic flow comparable to that of light mesons, implying collective motion of heavy quarks in the expanding medium, and, (b) a suppression at high transverse momentum (p_T) similar to light mesons, implying a substantial energy loss of fast heavy quarks while traversing the medium.

Several theoretical approaches have been put forward to describe heavy-quark energy loss, or, more generally, heavy-quark diffusion, in the QGP [11–24]. Two basic ingredients are required to perform quantitative calculations for the modifications of the initial spectra. On the one hand, one needs a good knowledge of the microscopic interactions of heavy quarks in the plasma, as encoded in their transport properties (drag and diffusion coefficients). On the other hand, one needs a realistic description of the expanding medium through which the heavy quarks propagate. The experimental spectra of heavy hadrons (and their decay electrons) only reflect a combination of both components. This may lead to ambiguities in disentangling the two ingredients.

A closer inspection of the theoretical modeling reveals differences in both macroscopic expansion scenarios and microscopic transport coefficients. A first comparison of these issues has been carried out in Ref. [25]. It is the purpose of the present article to separate both ingredients and study the influence of the medium description, the freeze-out prescription and the Langevin realization on the heavy-quark spectra. Here, we focus on two previously used medium descriptions, namely the hydrodynamical model by Kolb and Heinz [26], and the more schematic elliptical fireball model by van Hees et al. [12, 16].

The objective of this work is not to reproduce experimental data for heavy-flavor observables. Rather, we employ a common model for the elementary interaction but change the medium through which the heavy quarks propagate, or alternatively use a common description of the medium and change the elementary interaction, to elucidate the influence of both ingredients on the final spectra.

Our article is organized as follows: In Sec. II we describe the two medium descriptions used in our comparison and also briefly recall the main ingredients to each of the two transport calculations [12, 16, 23, 24]. In Sec. III we calculate the spectra for different combinations of transport coefficients and medium descriptions. In this way we can separate the influence of the expansion scenario from that of the elementary interaction of the heavy quarks with the plasma constituents. For definiteness, this comparison is conducted with the numerical (Langevin) implementation used in Ref. [23], but we also allude to the Langevin implementation as adopted

* Corresponding authors: pol.gossiaux@subatech.in2p3.fr, svogel@subatech.in2p3.fr

in Ref. [16]. In Sec. IV we elaborate on how light-quark observables, like the elliptic flow of pions, are constrained within the two expansion scenarios and can help to distinguish the latter. We conclude in Sec. V.

II. MEDIUM DESCRIPTIONS AND TRANSPORT COEFFICIENTS

Let us start by recalling the basic features of the medium expansion in Ref. [16], where an elliptical fireball has been used to model the evolution of the medium created in $b = 7$ fm Au+Au collisions at $\sqrt{s} = 200\,\mathrm{GeV}/c$, referred to as the vHR (van Hees/Rapp) medium in the following. It employs a QGP equation of state with $N_f = 2.5$ effective flavors which yields an entropy density

$$s_{\rm QGP}(T) = \frac{S}{V(t)} = \frac{4\pi^2}{90}(16 + 10.5N_f)T^3, \qquad (1)$$

with T being the temperature. The total entropy ($S \simeq 4600$ in $\Delta y = 1.8$ units of rapidity) is assumed to be time independent. The fireball volume is parametrized as a function of time according to

$$V(t) = \pi a(t)b(t)(z_0 + ct), \qquad (2)$$

with

$$\begin{aligned} a(t) &= a_0 + v_\infty\left[t - \frac{1-\exp(-At)}{A}\right] \\ &\quad - \Delta v\left[t - \frac{1-\exp(-Bt)}{B}\right], \\ b(t) &= b_0 + v_\infty\left[t - \frac{1-\exp(-At)}{A}\right] \\ &\quad + \Delta v\left[t - \frac{1-\exp(-Bt)}{B}\right]. \end{aligned} \qquad (3)$$

The tuning of the parameters,

$$\begin{aligned} &a_0 = 5.562\ \mathrm{fm},\ \ A = 0.55\,c/\mathrm{fm},\ \ b_0 = 4.450\ \mathrm{fm}, \\ &B = 1.3\,c/\mathrm{fm},\quad v_\infty = 0.52c,\qquad \Delta v = 0.122c\,, \end{aligned} \qquad (4)$$

will be discussed below. Since the fireball is approximated as homogeneous, the thermodynamic variables only depend on time but not on position. Therefore, for a given volume evolution and total entropy, the temperature, pressure and energy density can be calculated as a function of time as

$$p = \frac{\pi^2}{90}(16 + 10.5N_f)T^4 - B_{\rm QGP}, \qquad (5)$$

$$\epsilon = Ts - p = 3\cdot\frac{\pi^2}{90}(16 + 10.5N_f)T^4 + B_{\rm QGP}, \qquad (6)$$

where the bag constant, $B_{\rm QGP} = 356\ \mathrm{MeV/fm}^3$, ensures the continuity of pressure through the mixed phase (as in the EOS-Q of Refs. [26, 27]). The phase transition is modeled by a standard mixed-phase construction at constant temperature, $T_c = 180$ MeV, with critical QGP and HG energy densities of $\epsilon_c^{\rm QGP} = 2.25\ \mathrm{GeV/fm}^3$ and $\epsilon_c^{\rm HG} = 0.82\ \mathrm{GeV/fm}^3$ (the latter following from a thermal hadron-resonance-gas model). The expansion parameters in Eq. (3) have been determined to mimic the time evolution of the hydrodynamical model of Ref. [27] but with final quark-momentum spectra and elliptic flow (v_2) adjusted to results of coalescence-model fits to empirical pion and kaon spectra [28]. Note that this absorbs the effects of a subsequent hadronic evolution. The effective quark mass has been set to $m_q = 0.3$ GeV, and the freeze-out prescription has been chosen consistent with the equilibrium (i.e., long-time) limit of the post-point Ito realization of the Langevin simulation for the heavy quarks within the vHR model,

$$f_{\rm ML}(x,\vec{p}) = \frac{1}{(2\pi)^3}\frac{p\cdot u(x)}{E}\exp\left[-\frac{p\cdot u(x)}{T(t)}\right] \qquad (7)$$

(cf. Appendix A for details). This function is reminiscent of the one obtained within the so-called Milekhin freeze-out prescription [29, 30] and will therefore be referred to as "Milekhin-like" in the following. In Eq. (7), $u(x)$ is the four-velocity vector field of the medium. In vHR the transverse flow field, $\vec{v}_\perp(t,\vec{x})$, is constructed with help of confocal elliptical coordinates in the transverse (x,y) plane, i.e.,

$$\vec{v} = \left(\frac{r}{r_B}v_b(t)\cos v, \frac{r}{r_B}v_a(t)\sin v, 0\right), \qquad (8)$$

where $v_a(t) = \dot{a}(t)$, $v_b(t) = \dot{b}(t)$, and

$$\begin{aligned} \vec{r} &\equiv (x,y) = (0.6a_0\sinh u\cos v, 0.6a_0\cosh u\sin v) \\ \vec{r}_B &\equiv (b(t)\cos v, a(t)\sin v)\,. \end{aligned} \qquad (9)$$

The expansion parameters in Eq. (3) produce final light-quark spectra with an average surface-flow velocity of $v_b(t_{\rm mix}) \simeq 0.55$ and total elliptic flow of $v_2 \simeq 5.6\%$, at the end of the mixed phase. Note that these parameters are designed to reproduce hadron observables, not necessarily the result of a hydrodynamic model at the end of the mixed phase.

The second model to describe the expansion of the medium is (2+1)D hydrodynamical calculation by Kolb and Heinz (labeled KH) [26]. The equations underlying ideal hydrodynamics are the conservation of energy and momentum and appropriate currents (e.g., baryon number),

$$\partial_\mu T^{\mu\nu}(x) = 0\,, \quad \partial_\mu j^\mu(x) = 0. \qquad (10)$$

The equation of state is very similar to vHR, consisting of two parts. The hadronic phase is described as a gas of non-interacting hadronic resonances, containing essentially the same resonances as in the vHR fireball model but using a lower critical temperature, $T_c = 164$ MeV. Above the phase transition, in the QGP phase, the system is modeled as a non-interacting gas of u, d, s quarks

and gluons, with an external bag pressure (of a similar value as the one used in vHR). The temperature and energy density are local quantities in this approach. For more information on the modeling of the system with this approach the reader is referred to Ref. [26].

The parameters of both medium descriptions have been fixed to describe Au+Au collisions at $\sqrt{s}$ = 200 AGeV at an impact parameter of $b = 7$ fm. Note that the hydrodynamical model describes the hadron-p_T spectra and v_2 at thermal freeze-out in the hadronic phase, while the vHR fireball has been tuned to reproduce quark-momentum distributions at the end of the mixed phase such as to reproduce hadronic spectra within a coalescence model for hadronization [28]. Thus, by construction, the elliptic flow, v_2, in the vHR scenario is larger than in the KH scenario.

In Fig. 1 we display the temperature-time profiles extracted from KH hydrodynamics and the vHR fireball. In the hydrodynamical simulation the temperature is local, and for this comparison we take the temperature in the central cell. The temperature in the elliptic fireball depends only on its volume and is equal at all points in space. The vHR medium prescription starts at $\tau_0 = 0.33$ fm/c and stops at roughly 5 fm/c with the end of the mixed phase. For the KH prescription the medium evolution lasts longer, starting at $\tau_0 = 0.6$ fm/c and ending the mixed phase at ~ 7 fm/c, followed by a hadronic phase. The impact of the hadronic phase on the heavy-quark energy loss has been neglected when using the KH medium.

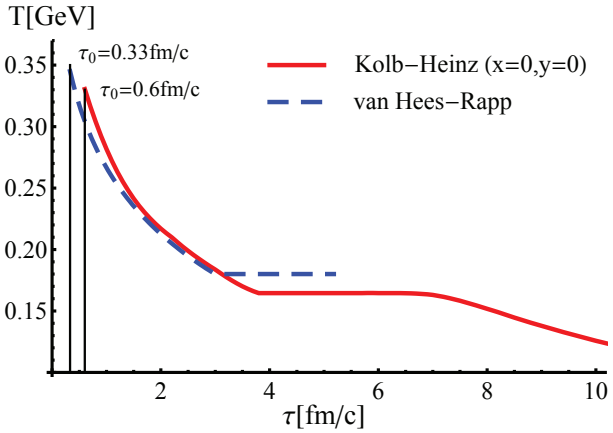

FIG. 1. (color online) Temperature profiles for KH hydrodynamics (central cell) and for the vHR elliptical fireball. One observes different lifetimes of the QGP and mixed phases for both approaches. Additionally, the hadronic phase of the KH description is depicted but heavy meson interactions are neglected.

Next we turn to the different descriptions of heavy-quark diffusion. In Refs. [23, 24] a pQCD calculation with running coupling has been used, whereas in Ref. [16] matrix elements based on an effective resonance model [12] have been employed. For this study, the interactions are implemented through the use of a Langevin-transport

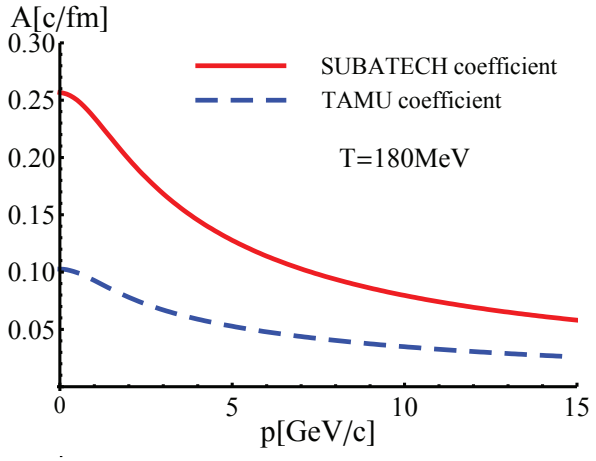

FIG. 2. (color online) Drag coefficients for pQCD with running α_s (solid line) and for resonance+pQCD interactions (dashed line), as a function of momentum for a temperature of 180 MeV. A clear difference between the two approaches is observed.

model (cf. Appendix A for more details) characterized by ensembles of random momentum kicks,

$$\mathrm{d}p_j = -\Gamma(t,\vec{p})p_j\mathrm{d}t + \sqrt{\mathrm{d}t}C_{jk}(t,\vec{p}+\xi\mathrm{d}\vec{p})w_k \ , \qquad (11)$$

which shift the heavy-quark momentum at each time step, dt; the first term, $-\Gamma(t,\vec{p})p_j$, is a friction term, w_k are Gaussian-distributed random variables and the C_{jk} are related to the diffusion tensor, $\hat{B}$ (see appendix). The choice of $\xi \in \{0, 1/2, 1\}$ characterizes realizations of the Langevin process, known as pre-point Ito, Stratonovich and post-point Ito (or Hänggi-Klimontovich) relations, respectively. For a particle of mass, M, which is large compared to the temperature of the ambient medium, one has $\Gamma = A + O(T/M) \approx A$ independent of the realization, where A is the drag coefficient responsible for the energy loss of particle, defined from the microscopic interaction by

$$A = \frac{1}{2pE}\int\frac{d^3k}{(2\pi)^3 2k}\int\frac{d^3k'}{(2\pi)^3 2k'}\int\frac{d^3p'}{(2\pi)^3 2E'}n_i(k) \times (2\pi)^4\delta^{(4)}(p+k-p'-k')\frac{1}{d_i}\sum|\mathcal{M}_i|^2\ (p-p') \ . \qquad (12)$$

Figure 2 depicts the drag coefficients computed in terms of the scattering-matrix elements of the underlying microscopic model for the heavy-quark interaction as a function of three-momentum at a fixed temperature of $T = 180$ MeV for the resonance model of Ref. [12] and for the pQCD model of Refs. [23, 24] (dubbed TAMU and SUBATECH coefficients, respectively). One finds sizable differences by more than a factor of two.

III. SYSTEMATIC COMPARISON OF HEAVY-QUARK SPECTRA

In this section we analyze heavy-quark spectra and elliptic flow by combining both medium descriptions with both transport coefficients, as alluded to in the previous section. In particular, we also study the time evolution of the elliptic flow. This requires the identification of a suitable variable characterizing the time evolution. In the vHR medium the energy density and the evolution time are uniquely correlated, but such a definitive relation does not exist in the hydrodynamic approach. In the KH medium we terminate the interactions of a heavy quark in a fluid cell as soon as its energy density falls below the freeze-out energy density, $\epsilon_{\rm fo}$, and evaluate the heavy-quark spectra on the pertinent hyper-surface.

In Fig. 3 we show the total v_2 for c-quarks, defined by

$$v_2^{\rm tot} := \frac{\int p_T {\rm d}p_T {\rm d}\varphi \cos(2\varphi) \frac{{\rm d}^3N}{{\rm d}y p_T {\rm d}p_T {\rm d}\varphi}}{\int p_T {\rm d}p_T {\rm d}\varphi \frac{{\rm d}^3N}{{\rm d}y p_T {\rm d}p_T {\rm d}\varphi}} \ , \qquad (13)$$

as a function of different freeze-out energy densities, $\epsilon_{\rm fo}$, down to the last point, where still a fraction of QGP exists, $\epsilon_{\rm fo} = 0.45\,{\rm GeV/fm^3}$ in KH and $\epsilon_{\rm fo} = 0.82\,{\rm GeV/fm^3}$ in vHR. All curves are calculated with the same microscopic model for the heavy-quark transport coefficients (pQCD with running coupling) [23, 24][1], but with different medium evolutions and Langevin realizations. The full red line (with diamonds) depicts the KH hydro evolution with the pre-point Langevin, the dashed line (with triangles) the equivalent result for the vHR fireball, and the full blue line (with circles) the vHR medium with a post-point Langevin; the latter corresponds to the results of Refs. [16].

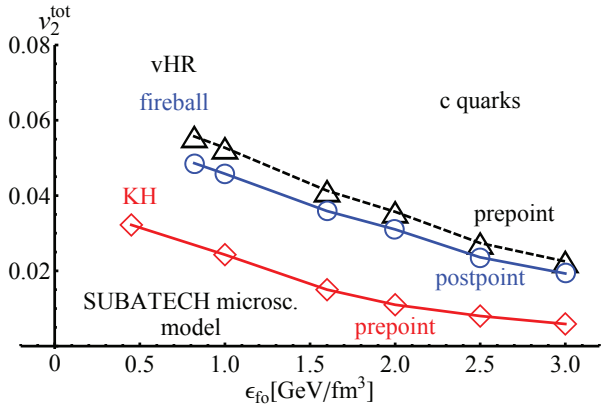

FIG. 3. (color online) Total v_2 of charm quarks as a function of freeze-out energy density for two different medium descriptions with identical (pre-point) Langevin realization (triangles and diamonds) and for the vHR evolution with post-point Langevin (circles).

We first note that the precise realization of the Langevin process has a moderate influence on the outcome of the calculation in the heavy-quark sector. For the two different medium descriptions, the discrepancies are larger, up to a factor of 2 at a given energy density. This suggests that both media carry different momentum eccentricities along their evolution[2], which, in turn, are transferred to the heavy-quark motion. We already pointed out that the vHR evolution has been tuned to the empirical v_2 of light quarks at the end of the mixed phase. We will return to this question in Sec. IV below; apparently, the moderate difference between 5.6% (vHR) and 4.8% (KH hydro) is not the main cause for the effect seen in Fig. 3.

In the following, we elaborate on how the differences in the medium expansion affect heavy-quark spectra by performing a comparison with different transport coefficients and medium prescriptions. Specifically, we compare two basic features of heavy-quark spectra at RHIC, i.e., the nuclear suppression factor, $R_{AA}(p_T)$, and the elliptic flow, $v_2(p_T)$, by studying four setups:

I. KH medium / SUBATECH coefficients

II. KH medium / TAMU coefficients

III. vHR medium / SUBATECH coefficients

IV. vHR medium / TAMU coefficients

The scenario described as "SUBATECH coefficients" are those published in Refs. [23, 24], whereas the drag and diffusion coefficients used in Refs. [12, 16] are labeled as "TAMU coefficients". The scenarios I and IV describe the published data on the nuclear suppression factor, R_{AA}, of semileptonic electrons fairly well, despite of different assumptions on the medium and the transport coefficients. To disentangle the effects of the two components, we swap the medium description with the description of the heavy-quark interaction (scenarios II and III). In this way we can cross-compare the results and better identify changes due to the medium or the diffusion mechanism. Since the precise realization of the Langevin process has rather little impact in the heavy-quark sector, we have chosen to proceed with the pre-point (post-point) prescription for the KH (vHR) medium; the motivation for this choice will be justified in Sec. IV.

Figure 4 depicts the nuclear suppression factor of charm quarks at the end of the respective mixed phases as a function of their transverse momentum for the four scenarios mentioned above. Scenarios I and IV give rather similar results, within ca. 20%. When changing the medium description and leaving the diffusion mechanism the same, i.e., comparing scenarios I with III, or II

[1] with the longitudinal coefficient B_L imposed as $B_L = TEA$ in order to enforce the Einstein relation.

[2] This feature, which we later on refer to as "intrinsic v_2" of the medium, could be further quantified by, e.g., evaluating the anisotropy, ϵ_p, of the energy-momentum tensor.

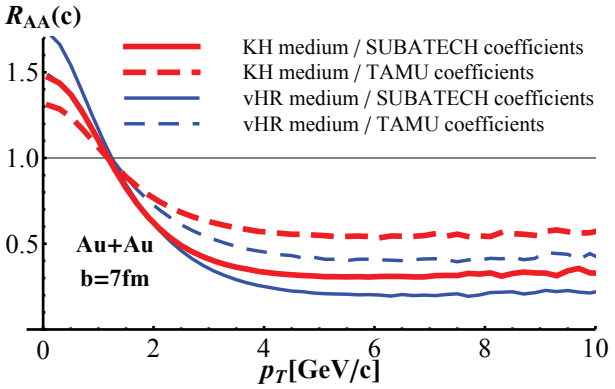

FIG. 4. (color online) Nuclear modification factor, R_{AA}, of charm quarks at RHIC energies for the four different scenarios. The lines are identified as scenario I (full/thick red), scenario II (dashed/thick red), scenario III (full/thin blue) and scenario IV (dashed/thin blue).

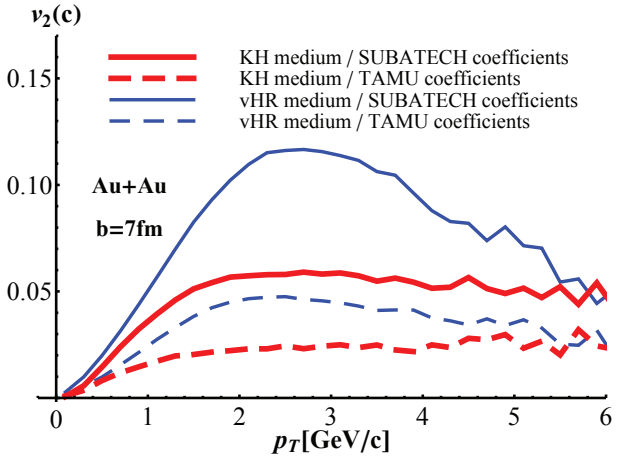

FIG. 5. (color online) Elliptic flow of charm quarks at RHIC energies. The red (blue) lines are computed with the KH hydro (vHR fireball) evolution, and the solid (dashed) correspond to using pQCD+running-α_s (resonance) model transport coefficients.

with IV, one observes a difference of 30-50% at high p_T in opposite directions, indicating that the vHR medium induces more "stopping" than the KH medium. As expected, the smaller friction coefficients of Refs. [12, 16] cause a smaller energy loss than the pQCD+running-α_s model. The maximal deviation of roughly a factor of 2 occurs when combining the large coefficients with the "more stopping" medium (scenario III) compared to the small coefficients plus "less stopping" medium (scenario II).

Similar features are found when comparing the elliptic flow of charm quarks, $v_2(p_T)$, see Fig. 5. One observes again that scenarios I and IV compare reasonably well to each other, on the level of ca. 20-30%. However, when interchanging the medium description the elliptic flow either increases by more than a factor of 2 (scenario III compared to I) or decreases by roughly a factor of 2 (scenario II compared to IV) at $p_T \simeq$ 2-4 GeV. The differences at intermediate p_T are thus stronger for v_2 than for R_{AA}.

IV. ELLIPTIC FLOW OF LIGHT CHARGED PARTICLES

As mentioned above, the calculated R_{AA} and v_2 values of charm quarks cause ambiguities in quantitatively disentangling the effects of the expansion scenario from that of the microscopic interaction of heavy quarks in the QGP. It is therefore important to return to light-quark observables to better distinguish between different scenarios. Light-hadron observables depend on the final state of the expansion scenario but are independent of the interaction of heavy quarks with the plasma constituents. Thus they allow to scrutinize the description of the medium evolution if the freeze out description were unique, which is unfortunately not the case. A key observable is the elliptic flow of pions or charged particles.

In the following we study in more detail how our two bulk evolution models have been adjusted to experimental data.

We adopt the standard definition for the differential elliptic flow of a particle with mass, m,

$$v_2(p_T) := \frac{\int \mathrm{d}\varphi \cos(2\varphi) \frac{\mathrm{d}^2N}{p_T \mathrm{d}p_T \mathrm{d}\varphi}}{\int \mathrm{d}\varphi \frac{\mathrm{d}^2N}{p_T \mathrm{d}p_T \mathrm{d}\varphi}} \tag{14}$$

in terms of the single-particle momentum distribution function[3]

$$\frac{\mathrm{d}^2N}{p_T \mathrm{d}p_T \mathrm{d}\varphi} = \int \mathrm{d}y \frac{E\mathrm{d}^3N}{\mathrm{d}^3p}. \tag{15}$$

If the expanding medium is in local thermal equilibrium during the expansion the key question is, how to convert the fluid cells, characterized by a temperature and flow field, into a particle distribution.

In the KH hydro calculations (as in most other hydrodynamical models) the Cooper-Frye (CF) prescription [31] is employed to evaluate the momentum distributions of particles after freeze-out. It converts a thermal medium instantaneously into a momentum distribution given by

$$\frac{E\,\mathrm{d}^3N}{\mathrm{d}^3p} = \int \mathrm{d}\sigma_\mu\, p^\mu f(\vec{p}, T, u). \tag{16}$$

with the Boltzmann - Jüttner distribution,

$$f(\vec{p}, T, u) = \frac{1}{(2\pi)^3} \exp\left(-\frac{p \cdot u}{T}\right), \tag{17}$$

[3] The integration over rapidity, y, is performed to collect the flow of all light partons that are able to interact with the heavy quarks in the rapidity interval $\Delta y = 1.8$ inherent to the fireball.

where T and u are the temperature and four-velocity at thermal freeze-out below which no further interaction occurs, and σ_μ is the hypersurface at constant T (or energy density). In the following, we will consider this prescription to analyze quark spectra during the evolution of the QGP as well.

In the vHR fireball model, the Milekhin-like freeze-out prescription has been adopted. Since the medium is approximated as isotropic, the hypersurface corresponds to the entire ellipsoid volume defined by the condition

$$\frac{x^2}{b^2(t)} + \frac{y^2}{a^2(t)} \leq 1 \; ; \tag{18}$$

The four-velocity at time, t, and position, $\vec{x}_\perp$, is evaluated from Eq. (8). According to Refs. [31, 32] one thus has

$$\frac{\mathrm{d}^3N}{\mathrm{d}y p_T \mathrm{d}p_T \mathrm{d}\varphi} = \frac{E\mathrm{d}^3N}{\mathrm{d}^3p} = \int_\mathcal{V} \frac{\mathrm{d}V}{(2\pi)^3} \; E \; f_{\rm ML}\,(p,T,u) \; , \tag{19}$$

with $f_{\rm ML}$ defined in Eq. (7). In the following, we will also evaluate the fireball-v_2 with the CF prescription, by taking $f_{\rm ML} \to f$ in Eq. (19).

In Fig. 6 we display the differential v_2 for constituent quarks with a mass $m = 300$ MeV, emanating from the KH and vHR medium, using both the Cooper-Frye and the Milekhin-like descriptions for the latter. Since the heavy-quark evolutions are terminated in both media at the end of the mixed phase, we choose the corresponding hypersurfaces for comparison. It turns out that the KH+Cooper-Frye and vHr+Milekhin-like prescriptions are rather close up to $p_T \simeq 700$ MeV. This encompasses most of the bulk-particles in the medium (and most of the interactions of the heavy quarks occur with those soft partons). However, if one applies the CF freeze-out to the vHR fireball one finds that the parton v_2 is systematically above the KH+CF and the vHR+ML medium, even at low p_T (e.g., by almost a factor of 2 at $p_T \simeq 700$ MeV, where KH+CF and vHR+ML cross). This reiterates the evidence found in the context of the charm-quark v_2 in Sec. III that the v_2-content of the vHR medium is significantly larger than that of the KH medium.

It is furthermore instructive to examine the *total* particle v_2 according to Eq. (13) – averaged over rapidity as in Eq. (15) –, which is particularly suitable to illuminate time (or energy-density) dependencies. In Fig. 7 we display this quantity as a function of the freeze-out energy density for $m = 300$ MeV "partons" above the critical value (0.45 fm^{-3} and 0.82 fm^{-3} for KH and vHR, respectively) and for $m = 140$ MeV "pions" below.

In the KH medium, for $\epsilon \lesssim 1.4$ GeV/fm^3, the direct evaluation of v_2 from the physical fields (e.g. $T_{\rm KH}(\tau_B, \vec{x}_\perp)$) is hindered by numerical fluctuations inherent to $\nabla\tau_{\rm fo}(\vec{x}_\perp)$, where $\tau_{\rm fo}(\vec{x}_\perp)$ is the freeze-out Bjorken time for a given position in transverse space. We have therefore resorted to a direct Monte-Carlo sampling of the freeze-out hypersurface, Σ, in order to evaluate this quantity in a more robust way.

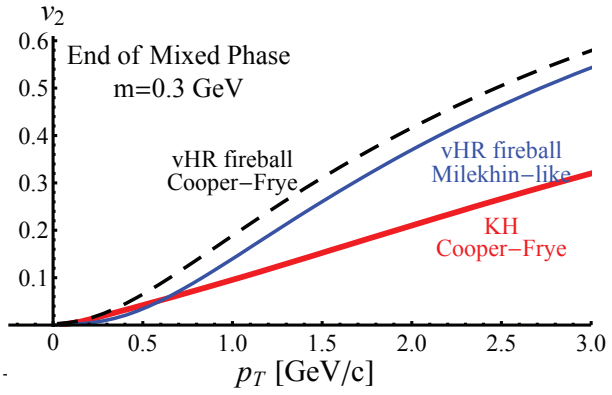

FIG. 6. (color online) Elliptic flow of particles with mass, $m = 300$ MeV, as a function of transverse momentum at the end of the respective mixed phase for the KH medium with Cooper-Frye freeze-out (solid red line) and the vHR medium+Milekhin-like freeze-out (solid blue line). The dashed line is the result of applying Cooper-Frye freeze-out to the vHR medium.

For the vHR fireball, there is no problem in performing the calculation for $v_2(\epsilon)$ down to the end of the mixed phase ($\epsilon_{\rm fo} = 0.82$ GeV/fm^3). By construction in the original work [16] the Milekhin-like freeze-out prescription results in an total v_2 of close to 6%, adjusted to experiment in semicentral Au-Au collisions at RHIC. The same is true for the KH-hydro+Cooper-Frye freeze-out, where, however, only 3/4 of the value is reached at the end of the mixed phase while the remaining 1/4 of the experimental value develops in the hadronic phase. Applying the CF freeze-out to the fireball leads to significantly larger values of ca. 9% at the end of the mixed phase, which is $\approx 60\%$ (90%) larger than the vHR+ML (KH+CF) prescriptions.

Pursuing the bulk evolution beyond the end of the mixed phase, one can compare the elliptic flow of directly produced pions, $v_2^{\rm tot}(\pi^+)$. In the case of the KH hydro, we have evaluated the v_2 directly from the π^+ spectra resulting from the hydrodynamical evolution. For the vHR medium, we have proceeded as described above for partons but simply taken $m = 140$ MeV and a Boltzmann distribution to resemble pions after the mixed phase. The resulting pion v_2 at the end of the mixed phase turns out to be 4.5% (8%) for Milekhin-like (CF) freeze-out, which is smaller (larger) than for the KH medium by roughly 25% (30%).

The analysis of the bulk v_2 summarized in Figs. 6 and 7 suggests an explanation for the origin of the discrepancies found in the charm-quark spectra analyzed in Sect. III: On the one hand, different freeze-out (and hadronization) prescriptions have been applied in the light-quark sector for the two medium descriptions, both of which lead to good agreement with the empirical pion v_2. On the other hand, when the two medium evolutions are analyzed with the same freeze-out prescription, an appreciable discrepancy in the bulk v_2 emerges. This "intrinsic" bulk v_2

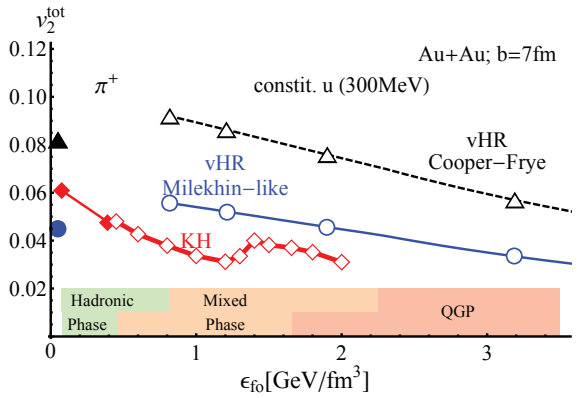

FIG. 7. (color online) Total v_2 as a function of freeze-out energy density for constituent quarks ($m = 300$ MeV, open symbols) and pions ($m = 140$ MeV, full symbols). The light quarks are evaluated with CF freeze-out for the KH (diamonds) and vHR (triangles) medium, as well as with the original Milekhin freeze-out for the vHR medium (circles). The colored boxes at the bottom sketch the three stages of the medium evolution (QGP, mixed and hadronic phase). The pions have been evaluated in the hadronic phase (using Boltzmann statistics, no resonance feeddown) either at the end of the mixed phase (vHR medium) or throughout the hadronic evolution for the KH medium.

appears to be the key quantity in communicating the momentum anisotropy to the heavy quarks propagating through the medium. Maybe somewhat surprisingly, the results in the heavy-quark sector, for "realistic" transport coefficients, are not very sensitive to the Langevin implementation (i.e., pre-point vs. post-point prescription), which, in turn, dictated the chosen freeze-out prescriptions in both media in the first place. Clearly, the theoretical issue remains to better understand the discrepancies in the different freeze-out descriptions in connection with the underlying Langevin implementation of heavy-quark diffusion, which of course should be consistent.

V. CONCLUSIONS

We have discussed the impact of the bulk-medium evolution on heavy-quark phenomenology in heavy-ion collisions by studying two expansion scenarios, which have been applied earlier to calculate the elliptic flow and nuclear suppression factor of heavy-quark observables at RHIC. In both approaches the final results depend on the microscopic interaction of the heavy quarks with the QGP (as encoded in their transport coefficients) and on the expansion scenario which provides different intrinsic v_2 values of the bulk medium. We separated these ingredients in order to better understand the influence of the medium descriptions on final spectra. By switching the medium and freeze-out descriptions one observes differences of around 50% in the R_{AA} and v_2 of charm-quark spectra. This effect has been cross-checked with different models for the microscopic input for drag and diffusion coefficients.

In the past, many efforts have concentrated on a better understanding of the microscopic interactions between heavy quarks and plasma constituents. Our study suggests that the influence of different expansion scenarios on the heavy-quark observables is comparable to that of different descriptions of the heavy-quark transport coefficients. In principle, light-quark observables can help to determine the expansion scenario but differences in freeze-out prescriptions and Langevin implementations induce significant uncertainties at present. Different freeze-out descriptions can indeed result in similar values for the light-meson v_2 in models where the "intrinsic" elliptic flow of the hot medium differs appreciably.

ACKNOWLEDGMENTS

The computational resources have been provided in part by Subatech. We acknowledge the support by U. Heinz for providing the hydrodynamical calculations and thank E. Bratkovskaya and R.J. Fries for fruitful discussions and comments. The work of RR and MH has been supported by the U.S. National Science Foundation under grant no. PHY-0969394 (RR, MH) and CAREER grant no. PHY-0847538 (MH), and by the A.-v.-Humboldt Foundation (RR). PBG, SV and JA have been supported by the ANR research program "hadrons@LHC" under grant no. ANR-08-BLAN-0093-02 and by the PCRD7/I3-HP program TORIC.

Appendix A: Langevin simulations and freeze-out scenarios

One of the difficulties in the use of relativistic Langevin simulations for heavy-quark diffusion processes is the dependence of the resulting phase-space distribution function on the realization of the stochastic integral. The Langevin process is defined by the time step,

$$\begin{aligned} \mathrm{d}x_j &= \frac{p_j}{E}\mathrm{d}t, \\ \mathrm{d}p_j &= -\Gamma(t,\vec{p})p_j\mathrm{d}t + \sqrt{\mathrm{d}t}C_{jk}(t,\vec{p}+\xi\mathrm{d}\vec{p})w_k \ , \end{aligned} \tag{A1}$$

for the heavy-quark position and momentum coordinates with respect to the rest frame of the heat bath. The $w_k(t)$ denote stochastically independent normally distributed random variables ("white noise"),

$$\langle w_j(t)w_k(t')\rangle = \delta(t-t')\delta_{jk} \ . \tag{A2}$$

As elaborated in Ref. [25], the Langevin process defined by Eq. (A1) is equivalent to the Fokker-Planck equation

$$\frac{\partial f}{\partial t}+\frac{p_j}{E}\frac{\partial f}{\partial x_j}=\frac{\partial}{\partial p_j}\left[\left(p_j\Gamma-\xi C_{lk}\frac{\partial C_{jk}}{\partial p_l}\right)f\right]+\frac{1}{2}\frac{\partial^2}{\partial p_j\partial p_k}(C_{jl}C_{kl}f)\ , \tag{A3}$$

for the heavy-quark phase-space distribution function f, where one can identify the usual drag force $A_j = p_j\Gamma - \xi C_{lk}\frac{\partial C_{jk}}{\partial p_l}$ as well as the diffusion tensor $\hat{B} = \hat{C}\cdot\hat{C}^T/2$. Here, $\xi \in [0,1]$ defines the realization of the stochastic integral, incorporating the effects of the force fluctuations around the average drag or friction force, governed by the drag coefficient, Γ. In Ref. [15], a pre-point Ito prescription has been adopted ($\xi = 0$), in which case one has identically $\Gamma = A$. Furthermore, the diffusion coefficients B_L and B_T have been adjusted to enforce the Einstein relation by solving Eq. (18) of Ref. [33] and imposing the additional constraint that

$$\frac{B_T(p)}{B_L(p)}=\left(\frac{B_T^{\rm brute}(p)}{B_L^{\rm brute}(p)}\right)^{\frac{1}{4}}\ , \tag{A4}$$

where $B_L^{\rm brute}$ and $B_T^{\rm brute}$ are the coefficients evaluated directly with help of the differential cross-section for the microscopic $q/g + Q \to q'/g' + Q'$ processes. This prescription has been adopted in order to preserve the anisotropy observed in high-energy collisions. Once these assumptions were adopted for the case of a fluid at rest, it has been checked numerically that the equilibrium limit of the distribution in a moving fluid is compatible with

$$f_{\rm BJ}(\vec{p}_{\rm lab})\propto\exp\left(-\frac{p_{\rm lab}\cdot u}{T}\right)\ , \tag{A5}$$

where $u = u(t,\vec{x})$ is the four-velocity flow field of the background medium with respect to the laboratory frame.

In Ref. [16, 19], following Ref. [13], the Langevin realization has been chosen so that heavy quarks reach thermal equilibrium in the long-time limit with the temperature given by the surrounding medium, leading to the Boltzmann-Jüttner distribution,

$$f_{\rm eq}(\vec{p})\propto\exp(-\sqrt{\vec{p}^2+m^2}/T)\ . \tag{A6}$$

To avoid the evaluation of momentum derivatives of the diffusion coefficients, the post-point Ito realization has been adopted for the stochastic integral ($\xi = 1$). This allows to set $\Gamma = A$ with the drag coefficient given by Eq. (12). As for the pre-point Ito, the longitudinal drag coefficient has been enforced to obey the Einstein-dissipation-fluctuation relation, $B_L = TEA$, with $E = \sqrt{m^2+\vec{p}^2}$, which indeed leads to the equilibrium limit, Eq. (A6), independently of the specific momentum dependence of the drag coefficient A [25]. For a flowing background medium, first the momentum coordinates have been Lorentz-boosted to the local heat-bath rest frame. After performing the time step (A1) in this frame, the new momentum variables have been transformed back to laboratory-frame coordinates. This procedure leads to an equilibrium limit

$$f_{\rm eq}(\vec{p}_{\rm lab})\propto\frac{p_{\rm lab}\cdot u}{E_{\rm lab}}e^{-\frac{p_{\rm lab}\cdot u}{T}}\ . \tag{A7}$$

In terms of a Cooper-Frye freeze-out description, Eq. (16), this corresponds to the choice of a hypersurface element $\mathrm{d}\sigma^\mu = \mathrm{d}^3x\ u^\mu$, which is similar to the modified Milekhin-freeze-out description discussed in Refs. [29, 30]. In order to render the thermal-fireball description of the bulk consistent with the freeze-out prescription implied by the equilibrium limit of the Langevin realization, the elliptic fireball described in Sec. II has been adjusted using Eq. (A7) as the local-equilibrium distribution of the light quarks. This leads to a light-quark bulk elliptic flow of $v_2 \simeq 5.6\%$, as shown by the endpoint of the Milekhin-like curve in Fig. 7. This value is compatible with the experimental v_2 for light hadrons when applying the coalescence model for hadronization of Ref. [28] (the same model has been subsequently used in Refs. [16, 19] to convert the heavy-quark spectra from the Langevin simulations into D- and B-meson spectra). As pointed out in the text, if instead the standard CF constant-lab time freeze-out prescription is used, for which $\mathrm{d}\sigma = \mathrm{d}^3x(1,0,0,0)$, the same fireball evolution leads to a higher bulk elliptic flow of $v_2 \simeq 9.2\%$ for light quarks of mass $m_q = 300$ MeV. This finding reiterates a main point of the present investigation: Conclusions about the microscopic dynamics (i.e, the transport coefficients of heavy quarks in the QGP) from experimental heavy-quark observables, like R_{AA} and v_2 of single electrons at RHIC, depend on the description of the expansion of the QGP. This expansion has to be understood from the light-hadron data.

[1] J. Adams *et al.* [STAR Collaboration], Nucl. Phys. A **757**, 102 (2005)
[2] K. Adcox *et al.* [PHENIX Collaboration], Nucl. Phys. A **757**, 184 (2005)
[3] B. B. Back *et al.*, Nucl. Phys. A **757**, 28 (2005)
[4] I. Arsene *et al.* [BRAHMS Collaboration], Nucl. Phys. A **757**, 1 (2005)
[5] W. A. Zajc, Nucl. Phys. **A805**, 283 (2008).
[6] B. Muller, Acta Phys. Polon. B **38**, 3705 (2007)

[7] S. Vogel, G. Torrieri, M. Bleicher, Phys. Rev. **C82**, 024908 (2010).

[8] W. Cassing, E. L. Bratkovskaya, Phys. Rev. **C78**, 034919 (2008).

[9] B. I. Abelev *et al.* [STAR Collaboration], Phys. Rev. Lett. **98**, 192301 (2007).

[10] A. Adare *et al.* [PHENIX Collaboration], Phys. Rev. Lett. **98**, 172301 (2007)

[11] B. Svetitsky Phys. Rev. D **37**, 2484 (1988)

[12] H. van Hees and R. Rapp, Phys. Rev. C **71**, 034907 (2005).

[13] G.D. Moore and D. Teaney, Phys. Rev. C **71** 064904 (2005).

[14] M. G. Mustafa, *Phys. Rev. C* **72**, 014905 (2005).

[15] P. B. Gossiaux, V. Guiho and J. Aichelin J. Phys. G **31**, S1079 (2005)

[16] H. van Hees, V. Greco and R. Rapp Phys. Rev. C **73**, 034913 (2006)

[17] N. Armesto, M. Cacciari, A. Dainese, C. A. Salgado and U. A. Wiedemann Phys. Lett. B **637**, 362 (2006)

[18] P. B. Gossiaux, V. Guiho and J. Aichelin J. Phys. G **32**, S359 (2006)

[19] H. van Hees, M. Mannarelli, V. Greco and R. Rapp, Phys. Rev. Lett. **100**, 192301 (2008)

[20] D. Molnar, J. Phys. G **31**, S421 (2005)

[21] B.W. Zhang, E. Wang and X. N. Wang, Phys. Rev. Lett. **93** (2004) 072301

[22] O. Linnyk, E. L. Bratkovskaya, W. Cassing, Int. J. Mod. Phys. **E17**, 1367 (2008).

[23] P. B. Gossiaux and J. Aichelin, Phys. Rev. C **78**, 014904 (2008)

[24] P. B. Gossiaux and J. Aichelin, J. Phys. G **36**, 064028 (2009)

[25] R. Rapp and H. van Hees, in R. C. Hwa and X. N. Wang (eds.), Quark-Gluon Plasma Vol. IV, World Scientific (2010) [arXiv:0903.1096 [hep-ph]].

[26] P. F. Kolb and U. W. Heinz, Quark Gluon Plasma, World Scientific, arXiv:nucl-th/0305084.

[27] P.F. Kolb, J. Sollfrank and U.W. Heinz, Phys. Rev. C **62** (2000) 054909.

[28] V. Greco, C.M. Ko and P. Levai, Phys. Rev. C **68** (2003) 034904.

[29] V. N. Russkikh and Yu. B. Ivanov, Phys. Rev. C **76**, 054907 (2007)

[30] Yu. B. Ivanov and V. N. Russkikh, Phys. Atom. Nucl. **72**, 1238 (2009)

[31] F. Cooper, G. Frye, Phys. Rev. **D10**, 186 (1974).

[32] F. Cooper, G. Frye, E. Schonberg, Phys. Rev. **D11**, 192 (1975).

[33] D.B. Walton and J. Rafelski, Phys. Rev. Lett. **84**, 31 (2000)